

In vitro and in silico Analysis Alnustone Induced Anticancer Effects in Human Gastric Cancer

Na Xu, Yixiu Zhao*

Department of Digestive Endoscopy Center, Central Hospital Affiliated to Shandong First Medical University, Jiefang Road, Jinan, CHINA.

ABSTRACT

Background: A growing number of people are at risk for gastrointestinal disorders due to dietary modifications and excessive consumption of processed food. Gastric Cancer (GC) ranks fifth in terms of frequency of diagnosis and is the third most common cause of cancer-related deaths worldwide. **Objectives:** The current work demonstrated the anti-cancer potential of Alnustone against stomach cancer in AGS cell lines. **Materials and Methods:** The cell viability study was performed to determine the IC₅₀ value for the Alnustone. The effect of Alnustone on the activity of Caspase-3, -8 and -9 was estimated by utilizing commercially available colorimetric assay kits. Also, molecular docking analysis was performed for the Caspase-3, -8, -9, BAX, BCL-2, and p53 to identify the interactions with the Alnustone. **Results:** The results depicted that treating the AGS cell line with Alnustone significantly increased the level of caspases, indicating the anti-cancer property of Alnustone. The molecular docking analysis has revealed a promising finding: Alnustone demonstrated a better interaction with Caspase-3 (Binding Affinity (BA)=-6.2 kcal/mol; RMSD=1.877Å) and Caspase-8 (BA=-6.1 kcal/mol; RMSD=1.092Å), surpassing its interaction with Caspase-9 (BA=-6.0 kcal/mol; RMSD=1.596Å) and BCL-2 (-6.6 kcal/mol; RMSD=2.5Å) based on the number of interacted hydrogen bonds. This suggests a potential strategy for the future: targeting Alnustone to enhance Caspase-3 activity, which could lead to a positive correlation with the expression of Caspase-8 (R=0.46; p-value=4e⁻²⁴) and Caspase-9 (R=0.27; p-value=1.1e⁻⁰⁸). However, Caspase-3 was negatively correlated with the expression of Bcl-2 (R=-0.014; p-value=0.77). **Conclusion:** The study results show that Alnustone is a strong contender for GC treatment since it induces apoptosis in AGS cells and exhibits a comparable correlation in *in silico* investigations.

Keywords: ADMET, Alnustone, Caspase, Gastric cancer, Molecular docking.

Correspondence:

Dr. Yixiu Zhao

Department of Digestive Endoscopy Center, Central Hospital Affiliated to Shandong First Medical University, Jinan, No. 105, Jiefang Road, Jinan-250013, CHINA.

Email: 18866811090@163.com

Received: 18-03-2025;

Revised: 04-06-2025;

Accepted: 21-08-2025.

INTRODUCTION

One significant ailment in the world is gastric cancer. Globally, stomach cancer is the sixth most common cancer to be diagnosed. GC ranks third among cancer-related fatalities due to its elevated mortality incidence and often terminal stage upon diagnosis.¹ There are two primary anatomical categories of gastric cancer: cardia gastric cancer and non-cardia gastric cancer. Both of these types have different risk factors and epidemiologic characteristics. Additionally, there are two histological subgroups of gastric cancer: the diffuse type, which is marked by ineffectively cohesive cells without a glandular pattern of proliferation, and the intestinal type, which has a glandular progress arrangement and includes adenocarcinomas.²

Reduced intake of vegetables and fruits that are fresh and excessive consumption of salt and certain classic salt-preserved meals are linked to an increased incidence of gastric cancer. Furthermore, a significant threat component for the occurrence of gastric cancer is *Helicobacter pylori*. Another significant external risk associated with gastric cancer is smoking.³ Initial gastric cancer typically exhibits no indications at all or is accompanied by generalized symptoms like dyspepsia. Terminal levels might include loss of weight, anorexia, and ongoing stomach discomfort. An incomplete set of symptoms might cause a postponed identification.⁴

As of right now, there is no gold accepted treatment for gastric or Gastroesophageal Junction (GEJ) cancer. The primary criteria used to choose a treatment regimen are the ailments stage, the existence of biomarkers, and the doctor's recommended course of action. The main treatments for gastric cancer are surgery, cytotoxic therapy, targeted therapy, and immunotherapies.⁵ Unfortunately, the majority of these treatments frequently have major negative consequences on healthy tissues and organs and are only successful when the condition is still in its early stages.



DOI: 10.5530/ijper.20261185

Copyright Information :

Copyright Author (s) 2026 Distributed under Creative Commons CC-BY 4.0

Publishing Partner : Manuscript Technomedia. [www.mstechnomedia.com]

Therefore, any suppressive or preventative measures would be essential.

The resistance of apoptosis is one of the defining characteristics of human malignancy. Both the onset and the end of apoptosis relies on the caspase protease series of enzymes. These caspases are separated into two groups: the caspases that carry out the destruction stage of apoptosis, known as executioner caspases (caspase-3, -6, and -7), and the initiator caspases (caspase-2, -8, -9, and -10), which are the initial ones to trigger in accordance to a signal.⁶ Scientific research on the usage of naturally occurring components, or micronutrients, and their powerful health advantages for humans has been conducted in several recent studies. It has been shown that chemicals originating from plants target different biological functions on a molecular level. Numerous illnesses, such as malignancies, inflammatory conditions like Cardiovascular Diseases (CVDs), ophthalmological disorders, arthritis, autoimmune diseases, etc., have been shown to benefit from phytochemicals as pharmaceuticals.⁷ Alnustone is a naturally occurring diarylheptanoid that is non-phenolic. It was initially separated and recognized from the *Alnus pendula* male flower. *Alpinia katsumadai* Hayata seeds and *Curcuma xanthorrhiza* Roxb rhizomes also be extracted from it.⁸

Previous research has demonstrated the anti-inflammatory, antiemetic, anti-hepatotoxic, and anticancer properties of Alnustone. Furthermore, a number of investigations have demonstrated that AKH seed extracts exhibited a wide range of biological properties, such as antibacterial, anti-inflammatory, antiviral and anticancer properties. According to recent research, Alnustone-components demonstrated strong anticancer activity towards the cancer cells MCF-7 for breast cancer and BEL-7402 for hepatoma.⁹ The main objective of the current study is to investigate the ant-tumor activity of Alnustone compound against AGS cell lines. The XTT test was used to measure the impact of Alnustone on cell viability. Caspases activity was measured by colorimetric method. In addition, the interaction of Alnustone with caspase was determined through *in silico* methodology.

MATERIALS AND METHODS

Cell culture

The human gastrointestinal cell line AGS (gastric-adenocarcinoma) was utilized in this investigation. The AGS cell line was cultivated in RPMI medium supplemented with 10% Fetal Bovine Serum (FBS), 100 IU/mL penicillin and 100 µg/mL streptomycin. The cultures were kept in a humidified CO₂ atmosphere with 5% humidity at room temperature.

Cell Viability Assay

An XTT-based assay kit was employed to evaluate the AGS cells viability. AGS cells were distributed into the 96 wells microtiter plate. Following that, the cells were cultured for duration of one day at a temperature of 37°C with 5% CO₂ to enable them to attach

themselves to the bottom of the wells. The microtiter plate was loaded with varied dose of Alnustone and incubated for 24, 48, and 72 hr. Following the completion of the relevant incubation time, 50 µL of the XTT reagent was administered to the plate and diluted until it reached a final concentration of 0.3 mg/mL. After then, the plate was incubated for two more hr. After incubation, a plate reader was used to measure the color complex's absorbance at 490 nm, with a reference wavelength set at 690 nm.

Estimation of Caspases activity

In order to offer additional substantiation of the Alnustone ability to induce apoptotic cell death, many apoptosis effectors were examined. By utilizing commercially available colorimetric assay kits we assessed the levels of Caspase-3, -8, and -9 in control and Alnustone treated AGS cell line with the IC₅₀ dose.

The dataset retrieval for molecular docking analysis

The targets such as Caspase-3 (PDB ID: 3DEI), Caspase-8 (PDB ID: 3KJQ), Caspase-9 (PDB ID: 3V3K), BAX (PDB ID: 4S0O), BCL-2 (PDB ID: 6GL8), and p53 (PDB ID: 1TUP) were retrieved from the Protein Data Bank (PDB) to carry out the molecular docking analysis.¹⁰⁻¹⁵

Preparation of protein structures and ligands

The protein structures of Caspase-3, Caspase-8, and Caspase-9 were retrieved from the PDB and pre-processed using Discovery Studio Visualizer (DSV) v19.1.0.18287 (www.accelerys.com). This involved removing water molecules and associated ligands. The Alnustone structure, obtained from the PubChem compound database in SDF format with 3D atomic coordinates provided,¹⁶ was then transformed into PDB format using DSV.

Molecular docking and Visualization

The molecular docking process was initiated for the defined targets, Caspase-3, Caspase-8, and Caspase-9, with Alnustone. This was done using Autodock Vina, an advanced tool with an integrated scoring algorithm integrated into PyRx software.¹⁷ This process predicts the most favorable binding modes between the targets and the ligand.

The Autodock vina uses a new scoring mechanism,

$$C = \sum_{i < j} f_{titj}(r_{ij}),$$

C-Sum of intermolecular and intramolecular distance; Σ -Over all of the pairs of atoms; f_{titj} -Symmetric set of interaction functions; r_{ij} -Interatomic distance.

The specified targets and ligands have been converted into PDBQT format. Using the PyRx virtual screening tool, we identified the active site residues interacting with the targeted

biomarkers. Additionally, the properties of the grid box were set to Caspase-3 (size_x=27.65 Å; size_y=23.61 Å; size_z=23.83 Å), Caspase-8 (size_x=25 Å; size_y=25 Å; size_z=25 Å), and Caspase-9 (size_x=21.39 Å; size_y=27.00 Å; size_z=24.56 Å). After running molecular docking simulations, we analyzed the targets' interactions with Alnustone in 3D and 2D using Discovery Studio Visualizer v19.1.0.1828, developed by Dassault Systèmes BIOVIA. This software is available at Rue Marcel Dassault, Vélizy-Villacoublay, France (URL: www.accelerys.com, Accessed on 9 July 2024). The toxicity properties of Alnustone were predicted using a ProTox 3.0 server (<https://tox.charite.de>).¹⁸

Correlation Analysis

We have analyzed the correlative expression of Caspase-3, -8, -9, and BCL-2 using the TCGA-STAD dataset by implementing the webserver Gene Expression Profiling Interactive Analysis 2 (GEPIA2) (<http://gepia2.cancer-pku.cn/>) to understand the expression pattern during stomach adenocarcinoma by implementing the Spearman correlation coefficient with the statistical significance of $p\text{-value} \leq 0.05$ which contains #408 tumor and #36 normal samples.¹⁹

Statistical Analysis

Three distinct samples' means and standard deviations were used to illustrate the findings. For the statistical evaluation, a one-way analysis of variance was employed. The Duncan's Multiple Range Test was the tool used to evaluate the variation between the variable groups. p value of less than 0.05 was considered substantial.

RESULTS

Cytotoxic effect of Alnustone in AGS Cells

To evaluate the antitumor impact on AGS cells, cells were treated with varying doses of Alnustone (0, 5, 10, 20, 40, 80, and 100 $\mu\text{M}/\text{mL}$) for 24, 42, and 72 hr using the XTT test. The results demonstrated that, dependent on concentration, Alnustone significantly inhibits cell proliferation. The IC_{50} (inhibitory concentration) of Alnustone for AGS cells was determined to be 53, 36, and 28 $\mu\text{M}/\text{mL}$ for triplicate investigations, as shown in Figure 1. We chose IC_{50} for more research based on our findings.

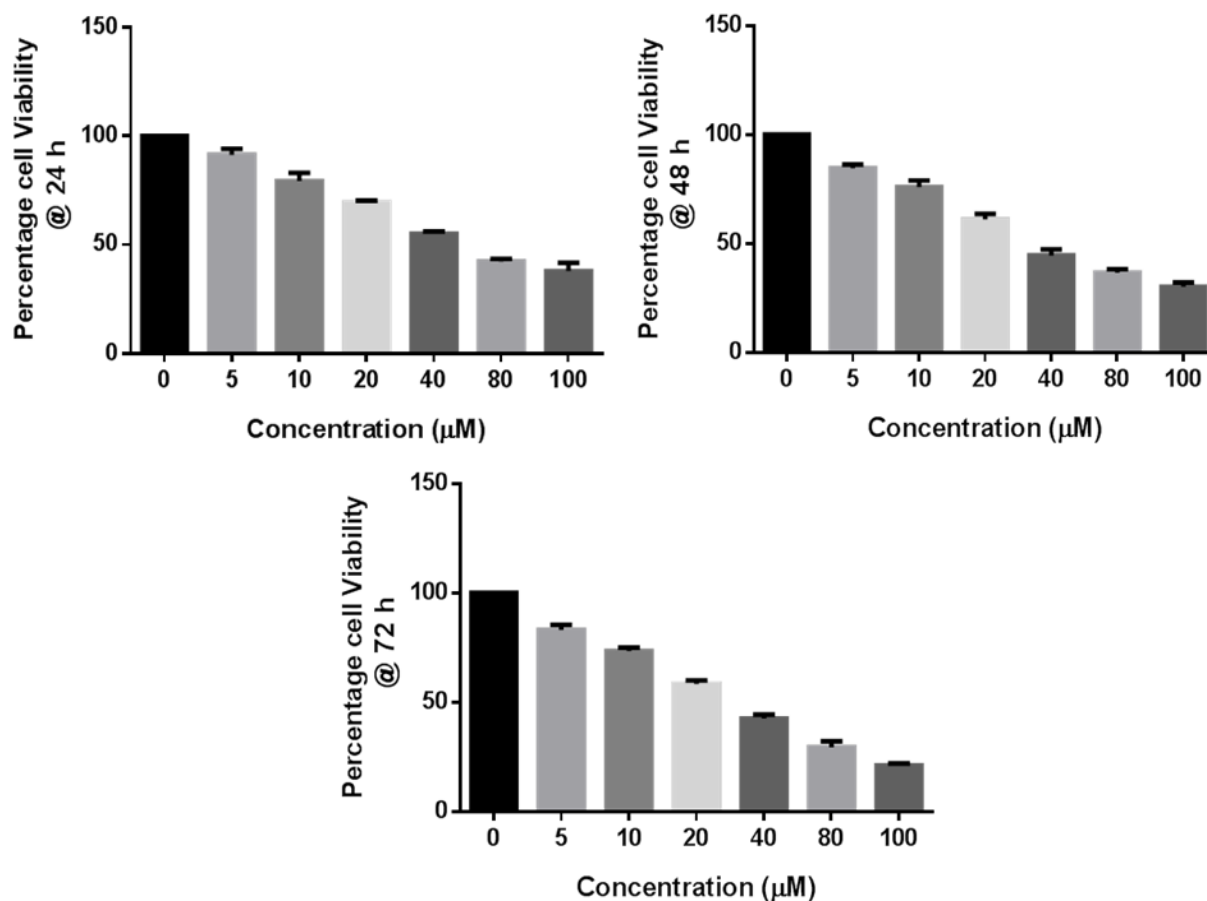


Figure 1: Effect of Alnustone on cell viability of the AGS cells by XTT assay. The results demonstrate that the treatment of Alnustone at different concentrations (0, 5, 10, 20, 40, 80 and 100 $\mu\text{M}/\text{mL}$) significantly inhibited the viability of AGS cells at 24, 48, and 72 hr time periods. Experiments were performed in triplicate to determine the IC_{50} value (24 hr 53 $\mu\text{M}/\text{mL}$, 48 hr 36 $\mu\text{M}/\text{mL}$, 72 hr 28 $\mu\text{M}/\text{mL}$) and representative data are shown here for the dose resulting in 50% inhibition of growth.

Potential of Alnustone on the level of caspase -3, -8, and -9

The caspase and Bcl-2 protein family, which comprises the pro-apoptotic Bax and caspase-9 proteins and the anti-apoptotic Bcl-2, is known to modify the mitochondria and produce early apoptotic cell changes. Alnustone-induced apoptosis in the AGS cells was confirmed by the detection of caspase enzymatic activity. Figure 2 illustrates the expression of the protein's caspase-3, caspase-8, and caspase-9 varies in treated and control cells. The level of caspase-3, caspase-8, and caspase-9 significantly increased in cells treated with Alnustone, indicating that Alnustone may have anti-carcinogenic properties. The mean±Standard Deviation of three distinct studies is displayed in the findings, with a **p*<0.05 difference from the control.

Bioinformatic results

The molecular docking analysis performed for the Caspase-3, -8, and -9 showed that Alnustone can interact with BCL-2 and Caspase-3 and more well than the Caspase-8, Caspase-9, BAX, and p53. The resulting binding affinity, RMSD, and the types of bonds formed between the Caspase-3, -8, -9, BAX, BCL2, and p53 with Alnustone were tabulated in Table 1.

Caspase-3

The Alnustone interacted with the residues of Caspase-3, including ASN208 and SER209, via the hydrogen bonds and with other residues, such as TRP214 and TRP206, via pi-alkyl and pi-pi-T-shaped bond. Also, the hydrophobic residues such as TYR204, ARG207, GLU246, PHE247, GLU248, SER251, and PHE256 were surrounding the Caspase-3Alnustone docked complex with the binding affinity of -6.2 kcal/mol and the RMSD of 1.877Å (Figures 3A, B and Table 1).

Caspase-8

Caspase-8 residue PHE355 interacted with the Alunstone via the hydrogen bond, and other residues such as ILE333, LYS353, and PHE355 bonded via the pi-alkyl and pi-pi T-shaped bonds. Also, the residues such as THR337, PHE340, VAL354, and GLN361 surrounded the Caspase-3 and Alnustone complex with a binding affinity of -6.1 kcal/mol and the RMSD of 1.092Å (Figures 3C, D and Table 1).

Caspase-9

The Alnustone interacted with residues such as CYS285, VAL338, TRP340, and TRP348 via pi-alkyl and pi-pi T-shaped bonds. Likely, the other residues, such as HIS237, SER339, ARG341,

Table 1: The Table detailed the list of targets, PDB ID, binding affinity (kcal/mol), RMSD (Å), and its interacted residues with the respective ligand Alunstone and its type of bonds.

Targets Name	Targets (PDB/UniProt ID)	Binding affinity (Kcal/mol)	RMSD (Å)	Hydrogen bond	Hydrophobic residues	Other bonds
Caspase-3	3DEI	-6.2	1.877	ASN208, SER209	TYR204, ARG207, GLU246, PHE247, GLU248, SER251, PHE256	TRP214 ^{PA, PPT} , TRP206 ^{PPT}
Caspase-8	3KJQ	-6.1	1.092	PHE355	THR337, PHE340, VAL354, GLN361	ILE333 ^{PA} , LYS353 ^{PA} , PHE355 ^{PPT}
Caspase-9	3V3K	-6.0	1.596	-	HIS237, SER339, ARG341, GLY381, ILE382, TYR383	CYS285 ^{PA} , VAL338 ^{PA} , TRP340 ^{PPT} , TRP348 ^{PPT}
Bax	4S0O	-5.7	2.464	-	PHE105, ASN106, TRP107, GLN155, SER163, PHE176	TRP151 ^{PPT} , TYR164 ^{PPS, PA} , VAL173 ^{PA}
Bcl-2	6GL8	-6.6	2.5	GLN118	PHE104, PHE112, MET115, LEU137	LEU119 ^{PA} , ARG129 ^{PA} , VAL133 ^{PA} , ALA149 ^{PA} , THR132 ^{PS} , PHE153 ^{PPS}
p53	1TUP	-5.9	2.747	-	PHE113, TYR126, ASN131, ASN268, SER269, PHE270,	ARG110 ^{AL} , LEU111 ^{PA} , TRP146 ^{PPS}

Note: PA-Pi Alkyl; PPT-Pi-Pi T-shap; PPS-Pi-Pi Stacked; PS-Pi-sigma; AL-Alkyl.

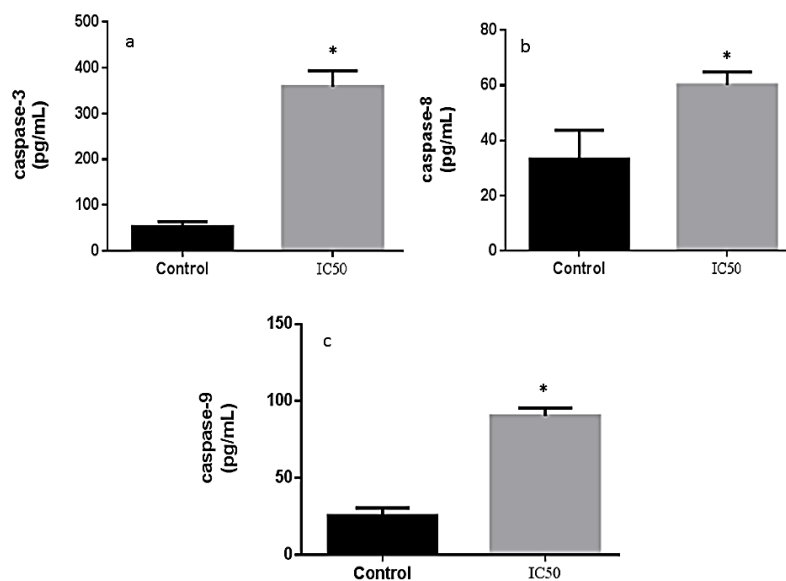


Figure 2: An assay kit based on colorimetry was used to assess caspase-3, 8 and 9 (a-c) activities in cell lysates. The data are revealed as a mean±SD of triplicates. *n*=3, **p*<0.005 compared to the control.

Table 2: The toxicity analysis of the Alnustone.

Compounds Name	Toxicity Analysis									LD ₅₀ (mg/kg)	TC
	Mutagenicity	Immuno toxicity	Hepato toxicity	Neuro toxicity	Respiratory toxicity	Cyto toxicity	Carcinogenicity	Clinical toxicity	BBB-barrier		
Alnustone	0.74 ⁽⁻⁾	0.86 ⁽⁻⁾	0.63 ⁽⁻⁾	0.66 ^(MA)	0.92 ⁽⁻⁾	0.95 ⁽⁻⁾	0.70 ⁽⁻⁾	0.65 ⁽⁻⁾	0.97 ⁽⁺⁾	2000	IV

Note: + indicates positive toxicity; - indicates negative toxicity; MA indicates Mild Active; A indicates Active.

GLY381, ILE382, and TYR383, surrounded the Caspase-9-Alnustone complex with the binding affinity of -6.0 kcal/mol and the RMSD of 1.596Å. However, no hydrogen bond is formed between the Caspase-9 and Alnustone (Figures 3E, F and Table 1).

BAX

BAX residues such as TRP151, TYR164, and VAL173 interacted via the Pi-Pi-T-shaped, Pi-Pi-Stacked, and Pi-alkyl bonds with the Alnustone. Also, hydrophobic interactions formed with the BAX residues, including PHE105, ASN106, TRP107, GLN155, SER163, and PHE176, with a binding affinity of -5.7 kcal/mol, and the estimated RMSD was 2.464Å. However, no hydrogen bonds formed between the Alnustone and BAX, exhibiting weak interactions (Figures 3G, H and Table 1).

BCL-2

The Alnustone formed the hydrogen bond with the BCL-2 residue GLN118. Likely, residues such as LEU119, ARG129, VAL133, ALA149, and PHE153 interacted with the Alnustone via Alkyl and Pi-alkyl bonds. Meanwhile, the THR132 interacted via the pi-sigma bond. Also, the hydrophobic residues such as PHE104, PHE112, MET115, and LEU137 surrounded the

BCL-2-Alnustone complex with a binding affinity of -6.6 kcal/mol and the RMSD was estimated as 2.5Å (Figures 3I, J and Table 1).

p53

In this, residues such as ARG110, LEU111, and TRP146 interacted via Alkyl, Pi-alkyl bonds with the Alnustone, and hydrophobic residues such as PHE113, TYR126, PHE270, SER269, ASN131, and ASN268 surrounded the complex with a binding affinity of -5.9 kcal/mol and the RMSD was estimated as 2.747Å (Figures 3K, L and Table 1).

The binding poses of Caspase-3 were validated through redocking, yielding a binding affinity of -6.4 kcal/mol and an RMSD of 1.508 Å (Figures S1 A, B). Similarly, the redocking approach confirmed the binding pose of Caspase-8 with a binding affinity of -6.1 kcal/mol and an RMSD of 0.66Å (Figures S1 C, D). The binding pose of Caspase-9 was also verified with a binding affinity of -6.0 kcal/mol and an RMSD of 1.596 Å (Figures S1 E, F). Furthermore, Alnustone interactions with BAX were confirmed through redocking, showing a binding affinity of -5.9 kcal/mol and an RMSD of 1.642 Å (Figures S1 G, H). The interactions of Alnustone with BCL-2 were reaffirmed with a binding affinity of -5.7 kcal/mol and an RMSD of 2.866 Å (Figures S1 I, J). Finally, redocking

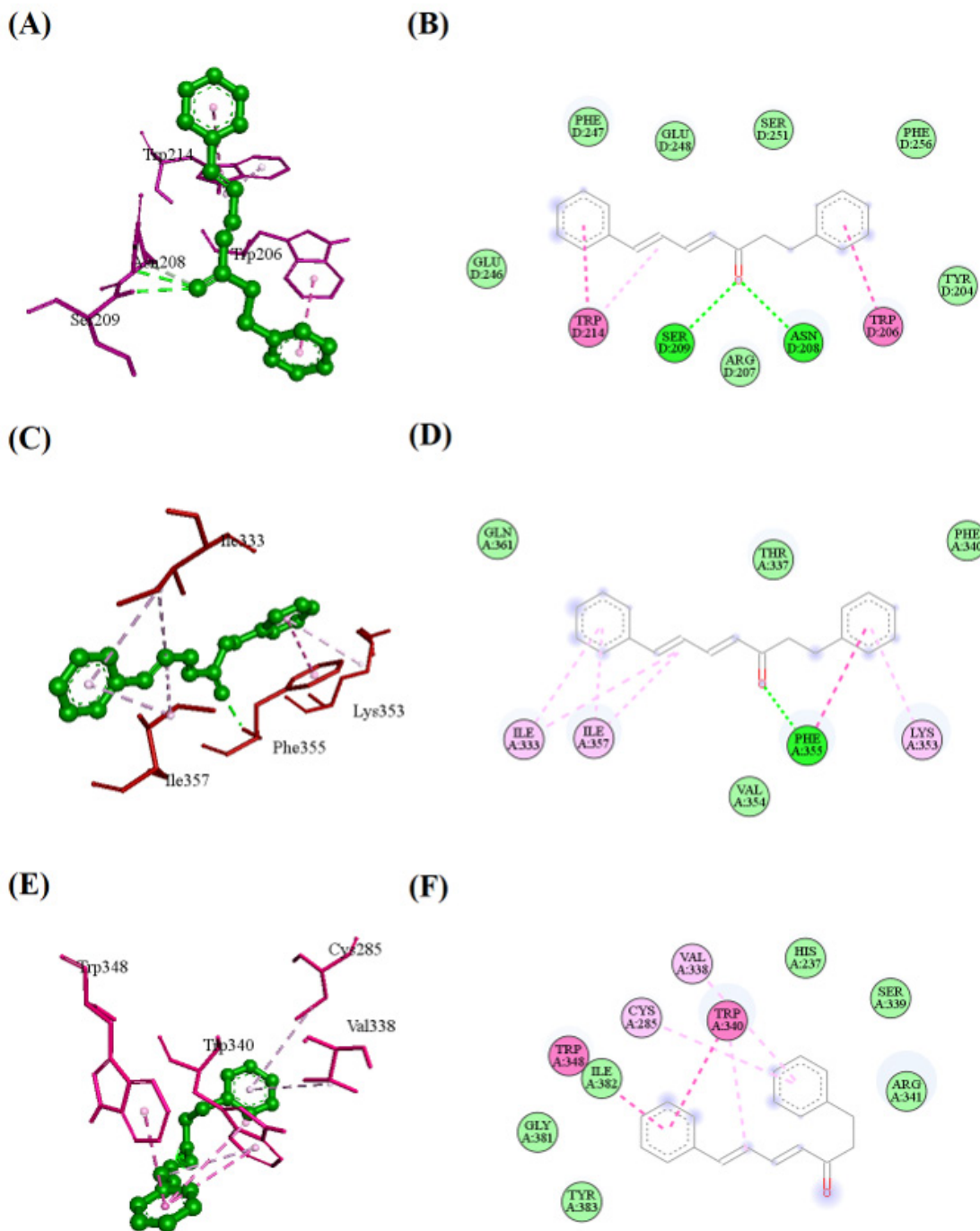
results validated the interaction of Alnustone with p53, revealing a binding affinity of -5.6 kcal/mol and an RMSD of 2.685 Å (Figures S1 K, L). Finally, the redocking further confirmed the docking results (Figures S1. A-L; Supplementary File).

The ADMET properties were evaluated for the Alnustone (Table 2), which revealed that the negative effect for the mutagenicity (0.74), immunotoxicity (0.86), neurotoxicity (0.66), respiratory toxicity (0.92), cytotoxicity (0.95), and carcinogenicity (0.70). Alnustone was found to have a predicted LD₅₀ of 2000 mg/kg, suggesting moderate acute toxicity and based on the LD₅₀,

the compound is classified as Class IV, indicating it has a low acute toxicity level, per the Globally Harmonized System of Classification and Labelling of Chemicals (GHS). However, it showed moderate hepatotoxicity (0.63) and BBB crossing ability (0.65).

Correlative expression of Caspase-3, Caspase-8, Caspase-9, and BCL-2

The molecular docking analysis beneficially showed the interactions among the Alnustone, Caspase-3, and Bcl-2. In this



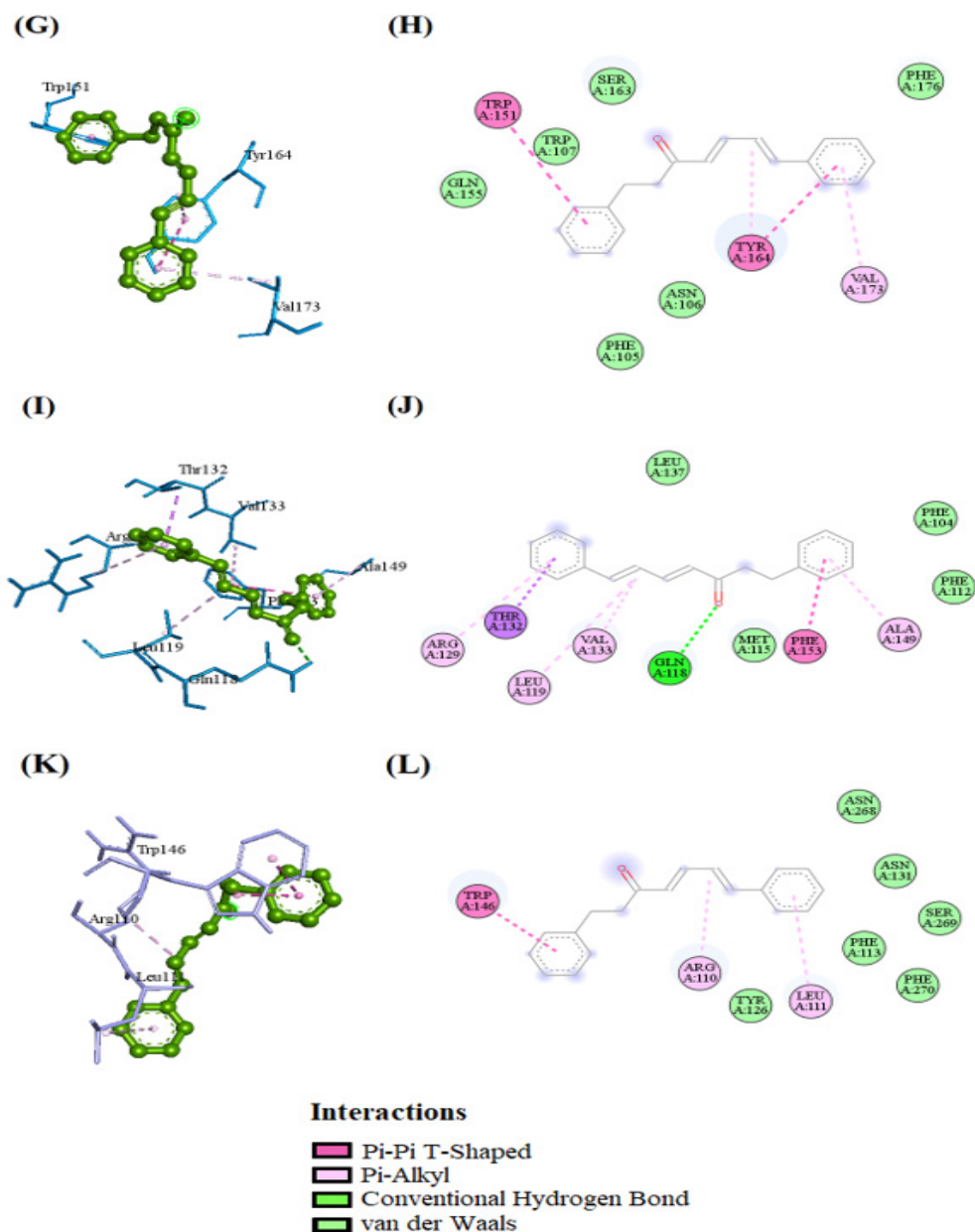


Figure 3: The docking pose of the selected targets Caspase-3 (PDB ID: 3DEI) (A, B), Caspase-8 (PDB ID: 3KJQ) (C, D), Caspase-9 (PDB ID: 3V3K) (E, F), Bax (PDB ID: 4S0O) (G, H), Bcl-2 (PDB ID: 6GL8) (I, J), and p53 (PDB ID: 1TUP) (K, L) with Alnustone.

context, the correlative expression for Caspase-8, -9, and Bcl-2 was analyzed against Caspase-3 (Figures 4A-C). The correlative expression analysis stated that the expression of Caspase-3 positively influenced the expression rates of Caspase-8 ($R=0.46$; $p\text{-value}=4e^{-24}$) and -9 ($R=0.27$; $p\text{-value}=1.1e^{-08}$) and ensured a significant statistical difference ($p\leq 0.05$) (Figures 4A-B). However, the CASP3 expression was negatively correlated with the BCL-2 ($R=-0.014$; $p\text{-value}=0.77$) without statistical significance (Figure 4C).

DISCUSSION

Over 1 million new cases of GC are reported globally annually, making it a major public health concern. GC is still the third most common source of cancer-related death globally, despite a drop in occurrence and death over the previous 50 years. GC is mostly caused by a persistent H pylori infection, which is responsible for around 89% of proximal gastric cancer cases globally. Further risk variables for stomach cancers were exposure to radiation, low-income countries, low levels of physical exercise, and tobacco use.²⁰ As of right now, advancements in the suppression of the growth of stomach cancer have included surgery. The therapeutic

impact is still not being met, nevertheless. Chemotherapy combined with cisplatin is a major therapeutic approach for gastric cancer in humans. Nevertheless, another significant barrier to cisplatin chemotherapy is resistance to drugs. Therefore, in order to avert stomach cancer and overcome medication resistance, efficient treatment options are required.²¹

Since natural anticancer medicines have few side effects and a great therapeutic potential, efforts have been concentrated on them during the past 10 years. The chemical structure of Alnustone, a nonphenolic diarylheptanoid, is mostly aryl-C7-aryl. Diphenylheptanes are said to have a variety of medicinal properties, including anti-inflammatory, antioxidant, hepatoprotective, and anti-tumor actions. Many actions, including antiemetic, anti-inflammatory, anti-hepatotoxic, antibacterial, anti-tumor, and mild estrogenic properties, are apparently displayed by Alnustone.²² Therefore, by investigating the function of Alnustone in gastric cancer, the current study aims to contribute to a better knowledge of the cancer development and to help in the development of treatment methods for gastric cancer.

Cell proliferation is a critical indicator of tumor development. Consequently, stopping the growth of a tumor mostly involves stopping malignant development by causing cancer cells to undergo apoptosis. In order to preserve cell homeostasis and throughout development and aging, apoptosis control is a crucial function. Apoptosis is a biological process that results in a distinct cell structure and eventual cell death.²³ Based on the results of the cell viability experiment, Alnustone considerably and dose-dependently impeded the growth of AGS cells. Alnustone's ability to suppress AGS cell division in this investigation so verified that it specifically inhibits cancerous growth.

The cysteine aspartic acid-specific protease family, which includes caspase-3 and caspase-9, is involved in the development of apoptosis in cancer.²⁴ Pro-caspase-3, an inactive version of caspase-3, is the original form of the protein. Caspase-8, Caspase-9, or Caspase-10 can initiate the transformation of Pro-caspase-3 to Caspase-3. Expression of caspase-3 indicates the effective suppression of tumor.²⁵ One of the most important regulators of apoptosis, which is a vital barrier towards hyper proliferation and cancer, is caspase-8. As a component of the intrinsic route, caspase-9 is triggered by cytochrome c release and mitochondrial injury. In the mitochondrial-initiated pathway, caspase activation is triggered by the formation of a multimeric Apaf-1/cytochrome c complex that is fully functional in recruiting and activating procaspase-9. Activated caspase-9 will then cleave and activate downstream caspases such as caspase-3, -6, and -7. This pathway is regulated at several steps, including the release of cytochrome c from the mitochondria, the binding and hydrolysis of dATP/ATP by Apaf-1, and the inhibition of caspase activation by the proteins that belong to the Inhibitors of Apoptosis (IAP).²⁶ Using calorimetric assay kit, the investigation evaluated caspase-8,

caspase-9, and caspase-3 levels. The results demonstrated that the AGS cells administered with Alnustone exhibited increased production of caspase-8, caspase-9, and caspase-3, indicating the activation of death in the cells. Furthermore, additional research is required to comprehensively recognize the mechanisms by which Alnustone demonstrates its therapeutic properties against GC.

The molecular docking analysis confirmed a more significant interaction between Caspase-3 and Alnustone than between Caspase-8 and -9 based on the number of hydrogen bonds (#2) involved. Also, the correlative gene expression analysis was performed to validate the expression of Caspase-3, -8, -9, and Bcl-2 and the results supported that Caspase-3 positively induced the expression of Caspase-8 and -9. The molecular docking analysis stated that Alnustone could trigger the expression of the Caspase-3/8/9 cascade against the GC, which might prevent cell proliferation. The ADEMT analysis demonstrated that Alnustone exhibited moderate hepatotoxicity and BBB crossing ability. It revealed that Alnustone required some structural modification that can be achieved by Pharmacophore technology in the future to hinder the BBB crossing ability to treat GC efficiently.

CONCLUSION

The present finding concludes that Alnustone can potentially inhibit gastric cancer by regulating the expression of caspase proteins. Alnustone was shown to considerably reduce the growth of AGS cells using the XTT assay, indicating that the molecule had a major impact in inducing apoptosis. The investigation assessed the expression of apoptotic proteins concerning Alnustone-treated cells. Comparing treated cells to untreated ones, it dramatically doubled the expression of caspase-3, caspase-8 and caspase-9. The molecular docking analysis confirmed better interactions between the Alnustone and key apoptotic proteins, particularly Caspase-3, with favorable binding affinity and increased hydrogen bonds. The correlation analysis demonstrated that Caspase-3 expression positively influenced the expression of Caspase-8 and -9, highlighting its central role in the apoptotic cascade. Moreover, Alnustone's interaction with the Bcl-2 family proteins, including pro-apoptotic Bax and anti-apoptotic Bcl-2, supports its potential to overcome resistance mechanisms often observed in GC treatment. The estimated toxicity properties stated that Alnustone exhibits a low-to-moderate toxicity profile with significant therapeutic potential. These results imply that, with more research, Alnustone may prove to be a highly successful anti-cancer medication for the efficient treatment of gastric cancer after validating with the *in vivo* experiments and clinical investigations.

CONFLICT OF INTEREST

The authors declare that there is no conflict of interest.

ABBREVIATIONS

GEJ: Gastroesophageal junction; **CVDs:** Cardiovascular diseases; **AGS:** Gastric adenocarcinoma; **XTT:** Methoxynitrosulphophenyl tetrazolium carboxanilide; **FBS:** Fetal Bovine Serum; **CO₂:** Carbon dioxide; **DSV:** Discovery Studio Visualizer; **PDB:** Protein Data Bank; **IC₅₀:** Half maximal inhibitory concentration; **GC:** Gastric cancer; **kcal:** Kilo calorie.

SUMMARY

The ameliorative action of Alnustone against AGS cells were thoroughly examined in this work. In the course of the study, Alnustone (IC₅₀ dosage) significantly increased the activity of caspase-3, -8 and -9 in the AGS cell line indicating the induction of apoptosis and anti-cancer property of Alnustone. Additionally, the molecular docking analysis revealed that Alnustone have better interaction with caspase -3 and caspase -9. Thus, it is anticipated that Alnustone will be utilized as a therapeutic drug for gastric cancer.

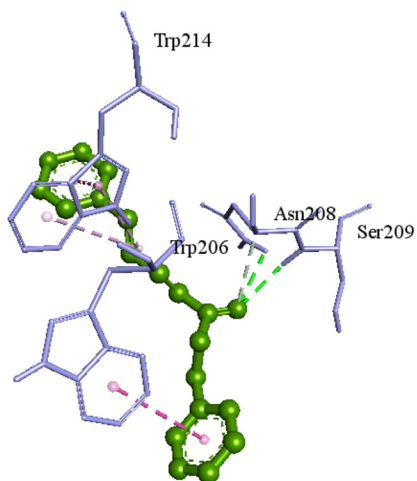
REFERENCES

- Smyth EC, Nilsson M, Grabsch HI, van Grieken NC, Lordick F. Gastric cancer. *Lancet*. 2020; 396(10251): 635-48. doi: 10.1016/S0140-6736(20)31288-5, PMID 32861308.
- Thrift AP, Wenker TN, El-Serag HB. Global burden of gastric cancer: epidemiological trends, risk factors, screening and prevention. *Nat Rev Clin Oncol*. 2023; 20(5): 338-49. doi: 10.1038/s41571-023-00747-0, PMID 36959359.
- Hartgrink HH, Jansen EP, van Grieken NC, van de Velde CJ. Gastric cancer. *Lancet*. 2009; 374(9688): 477-90. doi: 10.1016/S0140-6736(09)60617-6, PMID 19625077.
- Correa P. Gastric cancer: overview. *Gastroenterol Clin North Am*. 2013; 42(2): 211-7. doi: 10.1016/j.gtc.2013.01.002, PMID 23639637.
- Sexton RE, Al Hallak MN, Diab M, Azmi AS. Gastric cancer: a comprehensive review of current and future treatment strategies. *Cancer Metastasis Rev*. 2020; 39(4): 1179-203. doi: 10.1007/s10555-020-09925-3, PMID 32894370.
- Boice A, Bouchier-Hayes L. Targeting apoptotic caspases in cancer. *Biochim Biophys Acta Mol Cell Res*. 2020; 1867(6): 118688. doi: 10.1016/j.bbamcr.2020.118688, PMID 32087180.
- Fallah M, Davoodvandi A, Nikmanzar S, Aghili S, Mirazimi SM, Aschner M, et al. Silymarin (milk thistle extract) as a therapeutic agent in gastrointestinal cancer. *Biomed Pharmacother*. 2021; 142: 112024. doi: 10.1016/j.biopha.2021.112024, PMID 34399200.
- Salari Z, Alavi M, Rezaii-Zadeh H, Bouyahya A, Alfergah A, Afsari Sardari S, et al. Alnustone: a review of its sources, pharmacology, and pharmacokinetics. *Curr Mol Pharmacol*. 2024; 17: e18761429252459. doi: 10.2174/0118761429252459231115060139, PMID 38284732.

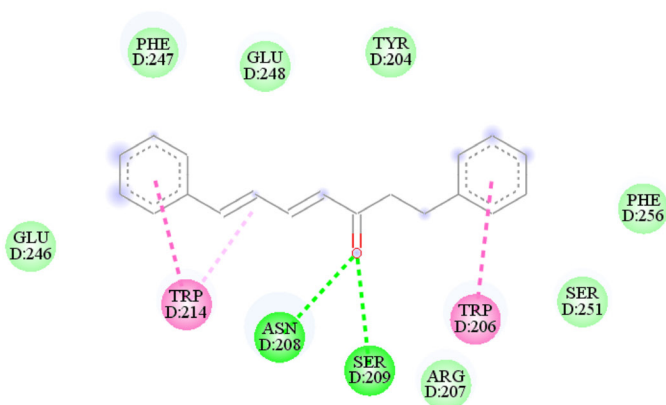
- Wang L, Cheng L, Ma L, Ahmad Farooqi A, Qiao G, Zhang Y, et al. Alnustone inhibits the growth of hepatocellular carcinoma via ROS-mediated PI3K/Akt/mTOR/p70S6K axis. *Phytother Res*. 2022; 36(1): 525-42. doi: 10.1002/ptr.7337, PMID 34847624.
- Du JQ, Wu J, Zhang HJ, Zhang YH, Qiu BY, Wu F, et al. Isoquinoline-1, 3, 4-trione derivatives inactivate caspase-3 by generation of reactive oxygen species. *J Biol Chem*. 2008; 283(44): 30205-15. doi: 10.1074/jbc.M803347200, PMID 18768468.
- Wang Z, Watt W, Brooks NA, Harris MS, Urban J, Boatman D, et al. Kinetic and structural characterization of caspase-3 and caspase-8 inhibition by a novel class of irreversible inhibitors. *Biochim Biophys Acta*. 2010; 1804(9): 1817-31. doi: 10.1016/j.bbapap.2010.05.007, PMID 20580860.
- Uchiyama R, Tsutsui H. Caspases as the key effectors of inflammatory responses against bacterial infection. *Arch Immunol Ther Exp (Warsz)*. 2015; 63(1): 1-13. doi: 10.1007/s00005-014-0301-2, PMID 25033773.
- Garner TP, Reyna DE, Priyadarshi A, Chen HC, Li S, Wu Y, et al. An autoinhibited dimeric form of BAX regulates the BAX activation pathway. *Mol Cell*. 2016; 63(3): 485-97. doi: 10.1016/j.molcel.2016.06.010 [ePub]. Erratum in: *Mol Cell*. 2016; 64(2): 431. doi: 10.1016/j.molcel.2016.10.005, PMID 27768876, PMCID PMC4975667.
- Casara P, Davidson J, Claperon A, Le Toumelin-Braizat G, Vogler M, Bruno A, et al. S55746 is a novel orally active BCL-2 selective and potent inhibitor that impairs hematological tumor growth. *Oncotarget*. 2018; 9(28): 20075-88. doi: 10.18632/oncotarget.24744, PMID 29732004, PMCID PMC5929447.
- Cho Y, Gorina S, Jeffrey PD, Pavletich NP. Crystal structure of a p53 tumor suppressor-DNA complex: understanding tumorigenic mutations. *Science*. 1994; 265(5170): 346-55. doi: 10.1126/science.8023157, PMID 8023157.
- Kim S, Chen J, Cheng T, Gindulyte A, He J, He S, et al. PubChem 2023 update. *Nucleic Acids Res*. 2023; 51(D1):D1373-80. doi: 10.1093/nar/gkac956, PMID 36305812.
- Eberhardt J, Santos-Martins D, Tillack AF, Forli S, Auto Dock V. Auto Dock vina 1.2.0: New docking methods, expanded force field, and python bindings. *J Chem Inf Model*. 2021; 61(8): 3891-8. doi: 10.1021/acs.jcim.1c00203, PMID 34278794.
- Banerjee P, Kemmler E, Dunkel M, Preissner R. ProTox 3.0: a webserver for the prediction of toxicity of chemicals. *Nucleic Acids Res*. 2024; 52(W1):W513-20. doi: 10.1093/nar/gkac303, PMID 38647086, PMCID PMC11223834.
- Tang Z, Kang B, Li C, Chen T, Zhang Z. GEPIA2: an enhanced web server for large-scale expression profiling and interactive analysis. *Nucleic Acids Res*. 2019; 47(W1):W556-60. doi: 10.1093/nar/gkz430, PMID 31114875, PMCID PMC6602440.
- Thrift AP, El-Serag HB. Burden of gastric cancer. *Clin Gastroenterol Hepatol*. 2020; 18(3): 534-42. doi: 10.1016/j.cgh.2019.07.045, PMID 31362118.
- Wang ZH, Zhan-Sheng H. Catalpol inhibits migration and induces apoptosis in gastric cancer cells and in athymic nude mice. *Biomed Pharmacother*. 2018; 103: 1708-19. doi: 10.1016/j.biopha.2018.03.094, PMID 29864961.
- Song Y, Zhou Y, Yan XT, Bi JB, Qiu X, Bian, Y, et al. Pharmacokinetics and tissue distribution of Alnustone in rats after intravenous administration by liquid chromatography-mass spectrometry. *Molecules*. 2019; 24(17): 3183. doi: 10.3390/molecules24173183, PMID 31480657.
- Saralamma VV, Nagappan A, Hong GE, Lee HJ, Yumnam S, Raha S, et al. Poncirin induces apoptosis in AGS human gastric cancer cells through extrinsic apoptotic pathway by up-regulation of Fas ligand. *Int J Mol Sci*. 2015; 16(9): 22676-91. doi: 10.3390/ijms160922676, PMID 26393583.
- Tian YZ, Liu YP, Tian SC, Ge SY, Wu YJ, Zhang BL. Antitumor activity of ginsenoside Rd in gastric cancer via up-regulation of caspase-3 and caspase-9. *Pharmazie*. 2020; 75(4): 147-50. doi: 10.1691/ph.2020.9931, PMID 32295691.
- Huang KH, Fang WL, Li AF, Liang PH, Wu CW, Shyr YM, et al. Caspase-3, a key apoptotic protein, as a prognostic marker in gastric cancer after curative surgery. *Int J Surg*. 2018; 52: 258-63. doi: 10.1016/j.ijsu.2018.02.055, PMID 29501797.
- Budihardjo I, Oliver H, Lutter M, Luo X, Wang X. Biochemical pathways of caspase activation during apoptosis. *Annu Rev Cell Dev Biol*. 1999; 15(1): 269-90. doi: 10.1146/annurev.cellbio.15.1.269, PMID 10611963.

Cite this article: Xu N, Zhao Y. *In vitro* and *in silico* Analysis Alnustone Induced Anticancer Effects in Human Gastric Cancer. *Indian J of Pharmaceutical Education and Research*. 2026;60(1):374-82.

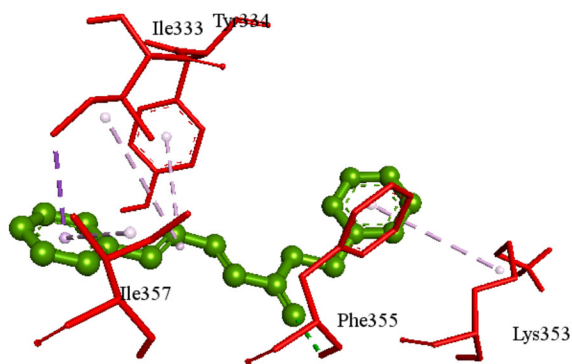
(A)



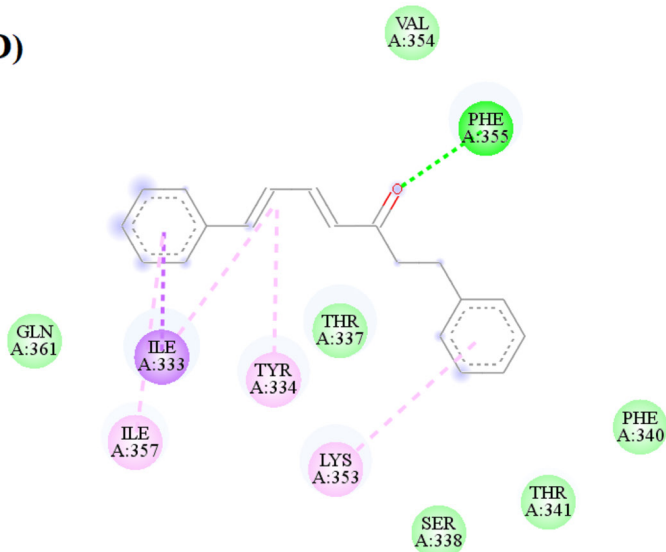
(B)



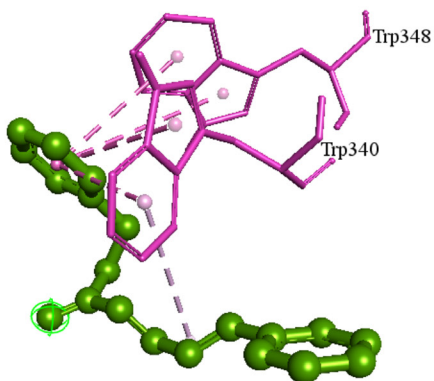
(C)



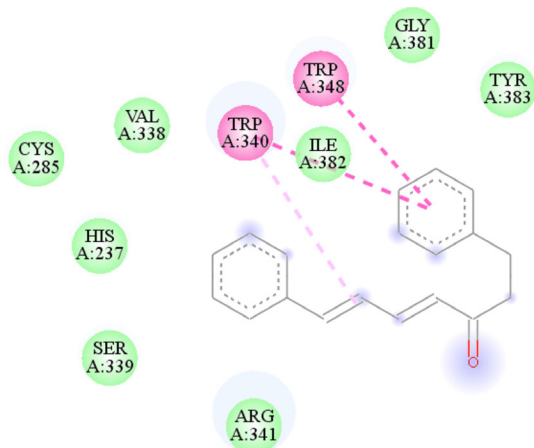
(D)



(E)



(F)



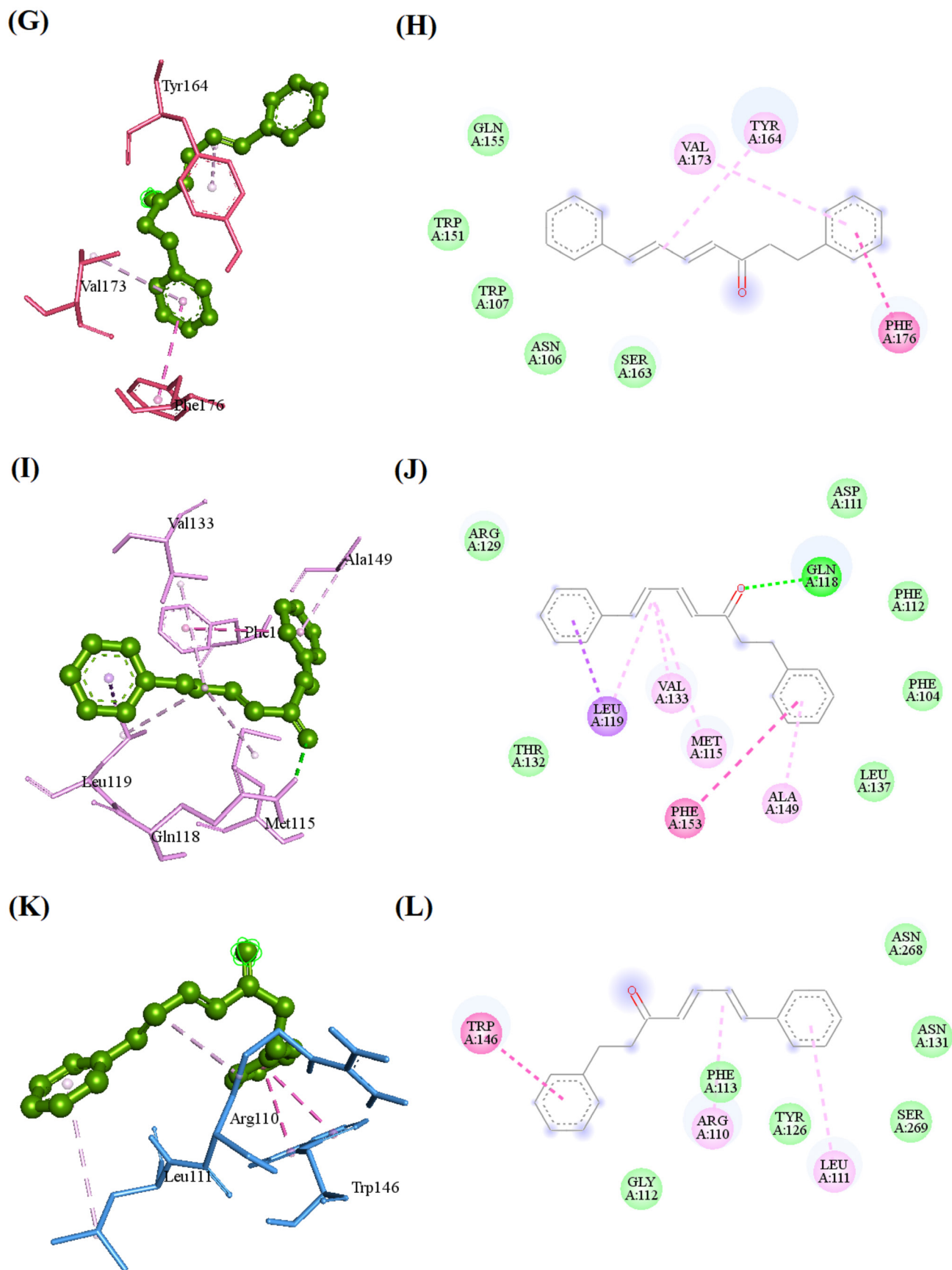


Figure S1: The redocking pose of the selected targets Caspase-3 (PDB ID: 3DEI) (A, B), Caspase-8 (PDB ID: 3KJQ) (C, D), Caspase-9 (PDB ID: 3V3K) (E, F), Bax (PDB ID: 4S0O) (G, H), Bcl-2 (PDB ID: 6GL8) (I, J), and p53 (PDB ID: 1TUP) (K, L) with Alnustone.